

## Vibrational properties of the amide group in acetanilide: A molecular-dynamics study

Alessandro Campa

*Theoretical Physics Department, The Rockefeller University, 1230 York Avenue, New York, New York 10021*

Andrea Giansanti and Alexander Tenenbaum

*Dipartimento di Fisica, Università degli Studi di Roma "La Sapienza," piazzale Aldo Moro 2, I-00185 Roma, Italy*

(Received 29 April 1986; revised manuscript received 7 May 1987)

A simplified classical model of acetanilide crystal is built in order to study the mechanisms of vibrational energy transduction in a hydrogen-bonded solid. The intermolecular hydrogen bond is modeled by an electrostatic interaction between neighboring excess charges on hydrogen and oxygen atoms. The intramolecular interaction in the peptide group is provided by a dipole-charge interaction. Forces are calculated up to second-order terms in the atomic displacements from equilibrium positions; the model is thus a chain of nonlinear coupled oscillators. Numerical molecular-dynamics experiments are performed on chain segments of five molecules. The dynamics is ordered, at all temperatures. Energy is widely exchanged between the stretching and the bending of the N—H bond, with characteristic times of the order of 0.2 ps. Energy transduction through the H bond is somewhat slower and of smaller amplitude, and is strongly reduced when the energies of the two bound molecules are very different: This could reduce the dissipation of localized energy fluctuations.

### I. INTRODUCTION

Around 1973 Davydov<sup>1</sup> proposed an energy transduction mechanism based on solitonic motions in the  $\alpha$  helixes of proteins. Yet in 1973 Careri<sup>2</sup> proposed acetanilide (ACN) as a relevant model system for the investigation of physical phenomena in natural polypeptides. Careri, Scott, and co-workers have recently explained an anomalous, low-temperature ir absorption band in ACN.<sup>3</sup> The firm assignment of this effect to a self-trapped state (Davydov-type soliton) of molecular vibrational energy in the amide group is a result of major relevance.<sup>4</sup> Moreover, the significance of this effect for the activity of an enzyme in a biochemical cycle has been recently explored by Careri and Wyman.<sup>5</sup>

We decided to investigate the molecular dynamics of ACN with the aim of exploring peculiar features of molecular energy exchange, possibly due to the nonlinearities of the hydrogen bonding. For this purpose we have set up a model of a segment of an ACN chain. We have selected few relevant degrees of freedom of the amide group (those involved in H bonding) and intentionally neglected the remaining ones in the molecule. Our aim was not to analyze a complete model of the ACN dynamics, but to search for a dynamical behavior that could be related to the solitonic localization of the energy, as found by Careri, Scott, and co-workers. Therefore, we considered only the degrees of freedom indicated as relevant by these authors:<sup>3,4</sup> the stretching of the C=O bond and the stretching and bending of the N—H bond.

Our model is classical; the use of classical mechanics in the study of atomic and molecular motions is valid if the thermal wavelength  $\lambda_T = \hbar/(2Mk_B T)^{1/2}$  of the atoms in the system is much shorter than the interatomic distances. This is the case for the present study. The potentials we used in this work seem to us sufficiently realistic, i.e., they

should have the same form in a quantum-mechanical treatment.

### II. THE MODEL

A pair of ACN molecules ( $\text{CH}_3\text{CONHC}_6\text{H}_5$ ) belonging to a chain is shown in Fig. 1, where we also show the set of coordinates we have used to describe the three degrees of freedom in each molecule of our model. The degrees of freedom refer to the oxygen ( $u$ ) and the hydrogen ( $\rho, \theta$ ) atom of the amidic group. Each molecule as a whole is kept fixed in its equilibrium position; we let the oxygen move along the C=O bond (C=O stretching), and the hydrogen atom can move along the N—H bond (N—H stretching) and transversely to the bond (N—H bending), remaining on the plane of the C=O...H—N group. Each atom vibrates around an equilibrium position, corresponding to a minimum of the potential energy. This motion, which is due to a restoring force generated by the presence of the other atoms in the same molecule and in the neighboring molecules is, to a first approximation, harmonic. There is also a peculiar interaction between

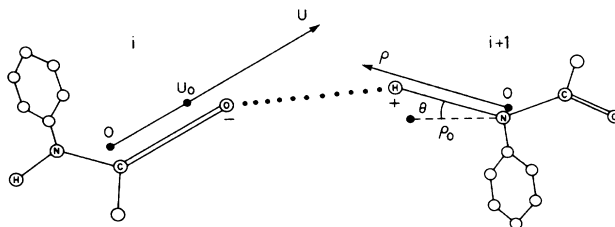


FIG. 1. Set of coordinates used in each ACN molecule.  $u_0$  is the equilibrium distance between C and O;  $\rho_0$  is the equilibrium distance between N and H;  $\theta=0$  at equilibrium. Numerical values are given in Table I.

TABLE I. Values of the constants in the expressions of the forces.

$q$	Excess charge on oxygen	$-1.5417 \times 10^{-10}$ esu
$q'$	Excess charge on hydrogen	$+4.8990 \times 10^{-11}$ esu
$u_0$	Equilibrium length of C—O bond	$1.2187 \times 10^{-8}$ cm
$\rho_0$	Equilibrium length of N—H bond	$1.0800 \times 10^{-8}$ cm
$r_0$	Equilibrium length of O...H bond	$1.8633 \times 10^{-8}$ cm
$d$	Half-length of C—N bond	$0.6767 \times 10^{-8}$ cm
$\cos\alpha$	Cosine [ $\pi - (\text{C}=\text{O} \cdots \text{H}$ angle)]	0.7564
$\sin\alpha$	Sine [ $\pi - (\text{C}=\text{O} \cdots \text{H}$ angle)]	0.6541
$M_1$	Oxygen mass	$2.6565 \times 10^{-23}$ g
$M_2$	Hydrogen mass	$1.6730 \times 10^{-24}$ g
$\omega_1$	Pulsation of the C=O stretching	$3.1384 \times 10^{14}$ sec $^{-1}$
$\omega_2$	Pulsation of the N—H stretching	$6.3146 \times 10^{14}$ sec $^{-1}$
$\omega_3$	Pulsation of the N—H bending	$3.0159 \times 10^{14}$ sec $^{-1}$
$a$	Longitudinal polarizability of C—N bond	$2 \times 10^{-24}$ cm $^3$

the oxygen and the hydrogen of the same amidic group: The movement of one of these two atoms generates a change in the charge distribution along the electronic structure of the group, which in turn exerts a force on the other atom. Furthermore, the hydrogen bond, which is the main intermolecular interaction, directly affects the degrees of freedom considered in our model. We therefore introduce three interactions: the restoring action of the medium, the intramolecular interaction that we have just described, and the intermolecular hydrogen bond. The total force acting on an atom in its equilibrium position being zero, we must subtract from the last two forces their equilibrium value. The dynamics is thus due to the harmonic restoring forces and to the change in the two other interactions which arises when the atoms move from their equilibrium positions.

#### A. Harmonic forces

We indicate with  $\bar{\nu}_1$ ,  $\bar{\nu}_2$ , and  $\bar{\nu}_3$  the values of the characteristic frequencies of C=O stretching, N—H stretching, and N—H bending, respectively. We choose typical values for these frequencies:  $\bar{\nu}_1 = 1665$  cm $^{-1}$ ,  $\bar{\nu}_2 = 3350$  cm $^{-1}$ , and  $\bar{\nu}_3 = 1600$  cm $^{-1}$ ,<sup>6</sup> and have the following expression for the harmonic potential energy of the  $i$ th molecule:

$$U_h^{(i)} = \frac{1}{2} M_1 \omega_1^2 (u_i - u_0)^2 + \frac{1}{2} M_2 [\omega_2^2 (\rho_i - \rho_0)^2 + \omega_3^2 \rho_0^2 \theta_i^2], \quad (2.1)$$

where  $\omega_i = 2\pi\bar{\nu}_i c$ , and  $u_0$  and  $\rho_0$  are the equilibrium lengths of C=O and N—H bonds, and  $M_1$  and  $M_2$  are the oxygen and hydrogen masses. By differentiation we can obtain the expressions of the harmonic forces. It should be noted that  $\theta$  being a rotation around an axis, when we differentiate with respect to  $\theta$  we get the momentum of the force relative to that axis. Nevertheless, we use a uniform notation ( $F$ ) for all the derivatives with respect to the coordinates. We get the following expressions for the harmonic forces acting on the  $i$ th coordinates:

$$\begin{aligned} F_{h,u}^{(i)} &= -M_1 \omega_1^2 (u_i - u_0), \\ F_{h,\rho}^{(i)} &= -M_2 \omega_2^2 (\rho_i - \rho_0), \\ F_{h,\theta}^{(i)} &= -M_2 \omega_3^2 \rho_0^2 \theta_i. \end{aligned} \quad (2.2)$$

We collect in Table I the values of all the constants used in our expressions.

#### B. Intramolecular interaction

The intramolecular interaction has been simulated by means of a dipole-charge interaction. In order to obtain a manageable expression we "straightened" the geometry of the peptide bond (see Fig. 2); we placed the O, C, N, and H atoms on a straight line, at mutual distances equal to those in the equilibrium configuration of the crystal. Excess charges were attributed to the oxygen and hydrogen atoms;<sup>7</sup> these charges generate in the middle of the C—N bond an electric field which, due to the polarizability of the bond, induces an electric dipole moment on it; the dipole field acts in turn on the charges. The C—N bond has an electric polarizability whose value is not exactly known; we have taken the value of  $2 \text{ \AA}^3$ , typical of many similar groups containing the carbon atom.<sup>8</sup> The dipole-charge (DC) force has been calculated with an expansion in powers of the atomic displacements from the equilibrium positions, up to second-order terms. Explicit expressions for the forces acting on the stretching of the oxygen ( $F_{\text{DC},u}^{(i)}$ ) and on the stretching of the hydrogen ( $F_{\text{DC},\rho}^{(i)}$ ) of

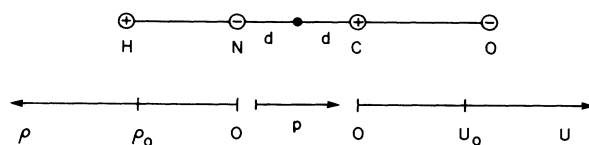


FIG. 2. Geometry adopted for the calculation of the dipole-charge intramolecular interaction. The C—N distance is  $2d$ .  $p$  is the dipole induced on the C—N bond by the charges on O and H; its sign in the expressions of the forces refers to the direction of the axis shown in the figure.

the  $i$ th molecule are given in Appendix A. We neglected variations of the excess charges during the motion of the atoms, because they would lead to corrections of higher order.

### C. Intermolecular hydrogen bonding

The intermolecular interaction is represented in our model by the hydrogen bond between the H atom in the N—H group and the oxygen atom of the carbonyl C=O group in the neighbor molecule. The hydrogen bond is best represented by an electrostatic interaction between charge excesses on nuclei plus a Lennard-Jones (LJ) interaction. The repulsive part of the LJ potential can be disregarded because the van der Waals radius of hydrogen in the N—H bond is negligible compared to the distance between this atom and the oxygen in the near molecule.<sup>9</sup> It is also possible to neglect the attractive part of the LJ potential, because it is weaker than the electrostatic interaction by at least 3 orders of magnitude, as can be easily estimated from the parameters given in Ref. 9 and from data in Table I. So we have modeled hydrogen bonding by a simple electrostatic interaction between the charge excesses of hydrogen and oxygen in two near molecules. Also in this case we used an expansion up to second-order

terms in the atomic displacements in order to calculate the forces due to hydrogen bonding:  $F_{\text{Hb},u}^{(i)}$ ,  $F_{\text{Hb},\rho}^{(i)}$ , and  $F_{\text{Hb},\theta}^{(i)}$ . In Appendix B we present the explicit expressions for these forces.

### D. Equations of motion

It is well known that the use of polar coordinates in a Lagrangian formulation leads to the appearance of velocity-dependent terms in the Lagrange equations. Taking these terms into account, the equations of motion for the  $i$ th molecule in our model are as follows:

$$\begin{aligned} M_1 \ddot{u}_i &= F_{h,u}^{(i)} + F_{\text{DC},u}^{(i)} + F_{\text{Hb},u}^{(i)} , \\ M_2 \ddot{\rho}_i &= F_{h,\rho}^{(i)} + F_{\text{DC},\rho}^{(i)} + F_{\text{Hb},\rho}^{(i)} + M_2 \rho_i \dot{\theta}_i^2 , \\ M_2 \rho_i^2 \ddot{\theta}_i &= F_{h,\theta}^{(i)} + F_{\text{Hb},\theta}^{(i)} - 2M_2 \rho_i \dot{\rho}_i \dot{\theta}_i . \end{aligned} \quad (2.3)$$

To have an estimate of the relative importance of the various terms in these equations we write them in a system of units in which the mean atomic displacements from equilibrium positions are of the order of unity. These units are  $10^{-10}$  cm for the lengths and  $2.5 \times 10^{-2}$  rad for the angles, and have been determined by equating the harmonic terms in (2.1) to  $k_B T$ , with  $T=100$  K. Collecting homologous terms in the equations, we get

$$\begin{aligned} \ddot{u}_i &= -9.8 \times 10^{28} (u_i - u_0) + 6.2 \times 10^{25} (\rho_i - \rho_0) + 6.6 \times 10^{25} (\rho_{i+1} - \rho_0) + 7.8 \times 10^{25} \theta_{i+1} \\ &\quad - 3.7 \times 10^{24} (u_i - u_0)^2 - 5.3 \times 10^{23} (\rho_i - \rho_0)^2 - 9.7 \times 10^{23} (u_i - u_0)(\rho_i - \rho_0) \\ &\quad + 5.3 \times 10^{23} (\rho_{i+1} - \rho_0)^2 - 4.2 \times 10^{24} \theta_{i+1}^2 + 5.1 \times 10^{23} (u_i - u_0)(\rho_{i+1} - \rho_0) \\ &\quad + 2.0 \times 10^{24} (\rho_{i+1} - \rho_0) \theta_{i+1} + 1.9 \times 10^{24} (u_i - u_0) \theta_{i+1} , \\ \ddot{\rho}_i &= -4.0 \times 10^{29} (\rho_i - \rho_0) + 9.8 \times 10^{26} (u_i - u_0) + 1.0 \times 10^{27} (u_{i-1} - u_0) + 1.2 \times 10^{24} (\rho_i - \rho_0)^2 \\ &\quad - 7.7 \times 10^{24} (u_i - u_0)^2 - 1.7 \times 10^{25} (\rho_i - \rho_0)(u_i - u_0) + 4.0 \times 10^{24} (u_{i-1} - u_0)^2 - 1.7 \times 10^{26} \theta_i^2 \\ &\quad + 1.7 \times 10^{25} (u_{i-1} - u_0)(\rho_i - \rho_0) + 3.1 \times 10^{25} (u_{i-1} - u_0) \theta_i + 6.2 \times 10^{-4} \rho_i \dot{\theta}_i^2 , \\ 10^{-4} \rho_i^2 \ddot{\theta}_i &= -1.1 \times 10^{29} \theta_i + 2.0 \times 10^{26} (u_{i-1} - u_0) + 2.4 \times 10^{24} (u_{i-1} - u_0)^2 \\ &\quad + 5.0 \times 10^{24} (u_{i-1} - u_0)(\rho_i - \rho_0) - 5.6 \times 10^{25} \theta_i (\rho_i - \rho_0) \\ &\quad - 1.3 \times 10^{24} (u_{i-1} - u_0) \theta_i - 2.0 \times 10^{-4} \rho_i \dot{\rho}_i \dot{\theta}_i . \end{aligned} \quad (2.4)$$

It is evident that in each equation the largest term is the first one; all other terms, linear and nonlinear, do not exceed a small percentage of the leading one. Notice that the term  $10^{-4} \rho_i^2$  in the last equation is of the order of unity in the new units. The period of the vibration of the hydrogen atom being of the order of  $2 \times 10^{-14}$  s, the velocity-dependent terms of the last two equations are of the same order of magnitude as the other perturbation terms. The smallness of the latter with respect to the harmonic term justifies the approximations we used in deriving them.

### E. Calculations

To integrate the equations of motion we used the well-known central differences algorithm.<sup>10</sup>

$$q_i(t+h) = -q_i(t-h) + 2q_i(t) + h^2 \ddot{q}_i(t) + O(h^4) ,$$

where  $q_i$  is a generalized coordinate ( $u, \rho, \theta$ ) of the  $i$ th molecule, and  $h$  is the integration time step. In our case we have to know the  $\dot{q}_i(t)$ 's to calculate  $q_i(t+h)$ , because there are velocity-dependent terms in the equations for  $\ddot{q}_i$  [see (2.3)]. To this end we have used a Taylor expansion up to second-order terms in  $h$ :

$$\dot{q}_i(t) = \dot{q}_i(t-h) + h \ddot{q}_i(t-h) + O(h^2) .$$

Using this expression in (2.3) does not affect the precision of the algorithm, which is still exact up to terms of the fourth order.

We considered the temporal courses of dynamical variables and their power spectra, computed by a

fast-Fourier-transform routine. The dynamical variables we considered were the coordinates  $u$ ,  $\rho$ ,  $\theta$ , and their energy, which, for each coordinate was the sum of the corresponding harmonic potential term in (2.1) and of a kinetic energy term, respectively  $\frac{1}{2}M_1\dot{u}^2$ ,  $\frac{1}{2}M_2\dot{\rho}^2$ , and  $\frac{1}{2}M_3\dot{\theta}^2$ ; the perturbative terms in the Hamiltonian were neglected. Our model was a chain of five molecules, numbered as in Fig. 1; the degrees of freedom of the first and the last molecule were kept fixed at their equilibrium value and the centers of mass of all the molecules were also kept fixed.

### III. RESULTS

In this section we give the results of our computer experiments; we say that an experiment was performed at temperature  $T$  if the total energy in the system was equal to  $k_B T$  times the number of degrees of freedom initially excited.

#### A. Short-time energy exchanges and anharmonicity

This section is based on the analysis of molecular dynamics runs of  $1.6 \times 10^5$  time steps; each time step being of  $5 \times 10^{-17}$  s, the total physical length of one of these runs was thus 8 ps. The first result we want to report here is that if energy is initially given only to a few degrees of freedom, for example to  $u_2$ ,  $\rho_3$ , and  $\theta_3$ , this energy will not spread, remaining confined in that region of the chain. In Fig. 3 the time course of the energy in the  $u_2$ ,  $\rho_3$ , and  $\theta_3$  coordinates is shown. This energy, equivalent to a temperature of 100 K, was initially given only to these degrees of freedom. Within the temporal range investigated the remaining degrees of freedom did not pick up any energy; and in fact the sum at any time of the energies reported in Fig. 3 gives a value equal to the total initial energy, showing no flux outside the initially excited region. Moreover, these degrees of freedom ex-

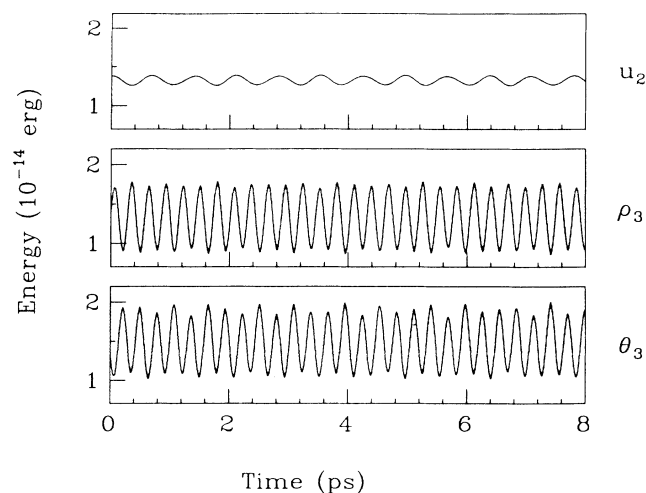


FIG. 3. Temporal course of the energy (kinetic plus potential) in the oxygen stretching  $u_2$ , in the hydrogen stretching  $\rho_3$ , and in the hydrogen bending  $\theta_3$ . Each of these degrees of freedom had initially an energy of  $1.38 \times 10^{-14}$  erg, corresponding to a temperature of 100 K.

change energy in a fairly regular, periodic way. The  $\rho_3$  and  $\theta_3$  coordinates exchange a large amount of energy between them; the energy initially given to the  $\rho$  vibration is passed to the  $\theta$  coordinate and then periodically regained. The exchange of energy initially given to the  $u$  coordinate is less pronounced, but still periodic, and this period is reflected as a modulation in the  $\rho$ - $\theta$  exchange.

When the energy given to the system is increased, the effect of the nonlinearities in the equations of motion also increases. We have calculated the power spectra of the energy in these degrees of freedom in several runs at different temperatures. The graphs show a very narrow peak at frequencies corresponding to the respective periods of energy exchange. In Fig. 4 we report these periods as a function of the temperature. It is evident that the period of energy exchange of  $u_2$  with  $\rho_3$  and  $\theta_3$  is constant and equal to 0.65 ps up to 350 K, then it decreases to 0.61 ps and this value is constant up to 700 K. The period (in ps) of energy exchange between  $\rho_3$  and  $\theta_3$  displays a temperature dependence which can be expressed by the relationship

$$\tau(T) = -0.0001313T + 0.3013,$$

as obtained by a linear regression on the data. These temperature effects are a clear manifestation of the nonlinearity of the system. From the power spectra of the coordinates we derived the temperature effect on the characteristic vibration frequencies of oxygen and hydrogen in our model; these frequencies appear as sharp peaks in the spectra, located around the typical values introduced in Sec. II. Figure 5 shows that the characteristic frequency of the  $u$  vibration is almost insensitive to the temperature and very close to the chosen value of  $1665 \text{ cm}^{-1}$ . It must be noticed that the expressions given in the Appendixes for the dipole-charge and hydrogen-bond forces acting on the degrees of freedom entail a first term which is harmonic and combines with the main harmonic term in the equations of motion (2.3). The modified harmonic terms correspond to characteristic frequencies which are easily

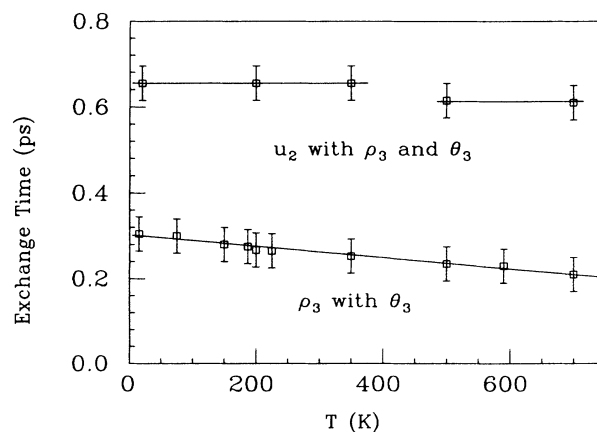


FIG. 4. Temperature dependence of the exchange periods as derived from power spectra of the energy in  $u_2$  (upper data), and in  $\rho_3$  (lower data; in these runs  $u_2$  was initially at rest). Solid lines are best fits.

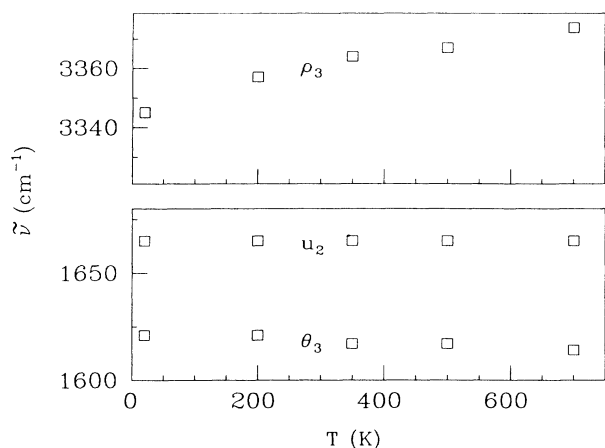


FIG. 5. Temperature dependence of the dominant vibration frequencies as derived from the power spectra of the three excited coordinates.  $\tilde{\nu} = \nu(\text{Hz})/c$ .

computable and turn out to be 1663, 3343, and 1617  $\text{cm}^{-1}$  for  $u$ ,  $\rho$ , and  $\theta$ , respectively. These frequencies are indeed found in the power spectra at low temperature, within the computational error. Figure 5 shows, however, that raising the temperature lowers slightly the vibration frequency of  $\theta$  (about  $0.01 \text{ cm}^{-1}/\text{K}$ ) and raises markedly the vibration frequency of  $\rho$  (about  $0.04 \text{ cm}^{-1}/\text{K}$ ), which is again a typical nonlinear effect.

We have investigated further features of the energy exchange between  $u_2$ ,  $\rho_3$ , and  $\theta_3$  as a function of temperature. In a series of runs we initially assigned energy only to  $\rho_3$  and  $\theta_3$ ; at each temperature we varied the fraction of the total energy initially given to the stretching  $\rho_3$ . In Fig. 6 the fraction of total energy periodically exchanged between stretching and bending is plotted as a function of the fraction of total energy initially present in the  $\rho_3$  coordinate. In all these runs the energy did not pass in any

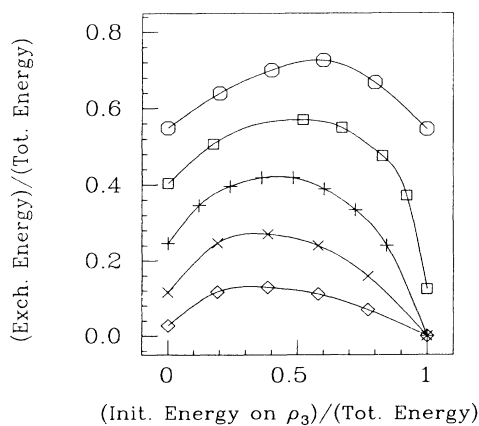


FIG. 6. Fractional energy periodically exchanged between stretching ( $\rho_3$ ) and bending ( $\theta_3$ ) of a N—H bond, as a function of the initial energy fraction in  $\rho_3$ ; all other coordinates were initially at rest. ( $\diamond$ ) 15 K, ( $\times$ ) 75 K, ( $+$ ) 225 K, ( $\square$ ) 590 K, ( $\circ$ ) 1200 K.

significant amount to the  $u_2$  or  $u_3$  coordinates, which were initially at rest. This is a general feature we have found in our runs: despite the presence of couplings, the dynamics of the initially excited degrees of freedom is not very much affected by the presence of other potentially available degrees of freedom, if these are initially at rest.

The effect of the nonlinearity is clearly shown in Fig. 6 by the temperature dependence of the curves. If we had a set of purely linear oscillators, changing the temperature would only rescale the energies; so all points in this plot, where fractional energies are reported, should lie on the same curve. But this is not the case. Let us also note the two extreme cases: when the whole energy is initially in the bending, this energy can be exchanged with the stretching apparently at all temperatures; but when the whole energy is initially in the stretching, exchange with the bending takes place only at quite a high temperature. This asymmetrical behavior too is a manifestation of the nonlinearities, as explored by increasing the temperature. There is a sort of threshold for the exchange of energy, when the energy is concentrated in the stretching; apart from a slight temperature effect, it is evident that the exchange is most efficient when the two degrees of freedom have about the same energy.

We performed also runs in which a fraction of the total energy was initially given to the  $u_2$  vibration, while  $\rho_3$  and  $\theta_3$  equally shared the remaining quantity. Figure 7 shows the amount of energy periodically exchanged by  $u$  as a function of the fraction of total energy initially given to it. No energy exchange takes place when the  $u_2$  coordinate on one side, or the  $\rho$  and  $\theta$  coordinates on the other are initially at rest; energy can be efficiently transferred through a hydrogen bond only if all the degrees of freedom are similarly excited. Thus at all temperatures there is a sort of exchange window, which favors energy transfer between molecules at similar temperatures and lowers energy transfer between "cold" and "hot" molecules. Further comments on Figs. 6 and 7 will be given in the concluding section.

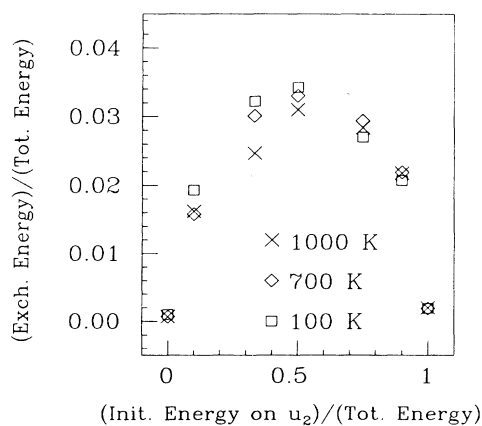


FIG. 7. Fractional energy periodically exchanged between a C=O bond ( $u_2$ ) and a N—H bond ( $\rho_3, \theta_3$ ) as a function of the initial energy fraction in  $u_2$ ;  $\rho_3$  and  $\theta_3$  equally shared the remaining energy at the beginning of the run.

The peculiar energy-exchange regime just described has a reflex also in the power spectra of the degrees of freedom. In Figs. 8(a) and 8(b) we report power spectra of the  $\rho_3$  coordinate when only this coordinate is initially excited. At the lowest temperature (i.e., 20 K) there is only a neat peak around the characteristic frequency of the N—H stretching near  $3350\text{ cm}^{-1}$ ; no other peak appears in the spectrum, indicating that the other degrees of freedom, initially at rest, do not affect the dynamics of the vibration we are considering. When the energy is 100 times higher (i.e., at 2000 K) the spectrum base line is raised by the same factor and numerous spectral lines grow up in the characteristic region around  $3350\text{ cm}^{-1}$ , but also below  $300\text{ cm}^{-1}$ . These low-frequency lines must be related to the energy exchange with the  $\theta$  vibration. A richer spectrum is displayed by the  $\rho_3$  coordinate when the initial energy is given also to  $u_2$  and  $\theta_3$  [Figs. 8(c) and 8(d)]. At low temperature the spectrum shows, beside the characteristic frequency of the N—H stretching, peaks around  $3240$  and  $1660\text{ cm}^{-1}$ . While the latter is clearly related to the coupling between  $\rho_3$  and  $u_2$ , the former corresponds to the second harmonic of the N—H bending and suggests a resonance between the two degrees of freedom of the H atom. There is also a small peak at low frequency, which indicates again that the dynamics of the N—H stretching is modulated by the slow energy exchanges. At high temperature numerous other lines appear in a picture indicating a transition to a different multiperiodic regime. Still the main lines can be attributed to the same mechanisms as at low temperature, if one takes into account the shift of the characteristic frequencies at high temperature (Fig. 5). So the peak around  $3400\text{ cm}^{-1}$  is the fundamental line of  $\rho_3$ , and the peak around  $3205\text{ cm}^{-1}$  is the second harmonic of  $\theta_3$ ; the peak corresponding to the coupling with  $u_2$  is almost unperturbed (as is the frequency of  $u_2$  when temperature changes), while the low-frequency region shows the growing weight of the slow energy exchanges. As we have already noticed the  $u$  vibration is more rigid in its en-

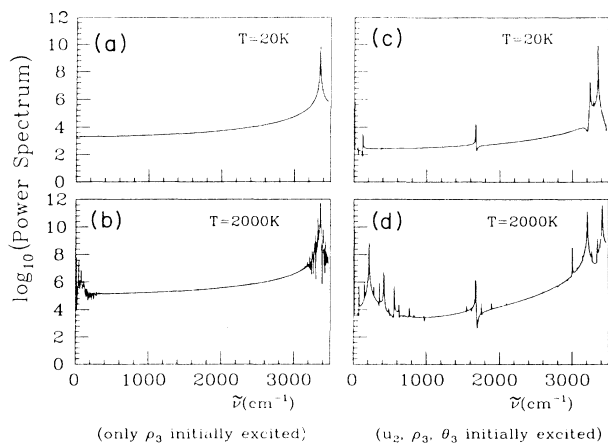


FIG. 8. Power spectra of the  $\rho_3$  vibration at different temperatures and initial conditions. Graphs on the right refer to runs in which  $u_2$ ,  $\rho_3$ , and  $\theta_3$  had the same energy; graphs on the left to runs in which only  $\rho_3$  was initially excited.

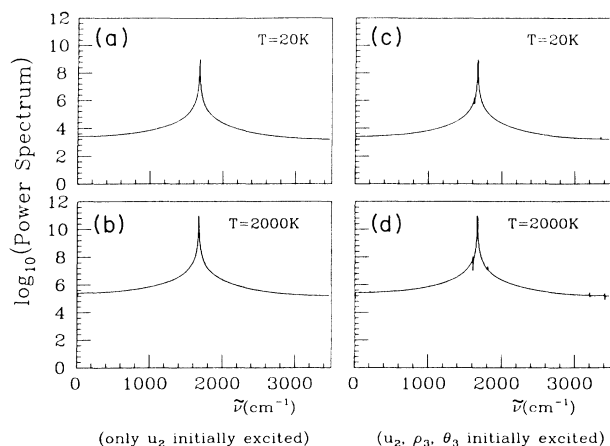


FIG. 9. Power spectra of the  $u$  coordinate at different temperatures and initial conditions. Graphs on the left refer to the  $u_2$  coordinate when only this one was initially excited. Graphs on the right refer to the  $u_2$  coordinate when  $u_2$ ,  $\rho_3$ , and  $\theta_3$  initially had the same energy.

ergy exchanges, and this is reflected in its power spectrum. The power spectra of the  $u_2$  vibration, when this is the only excited coordinate [Figs. 9(a) and 9(b)], are very similar to the spectra of the  $u_2$  coordinate when  $\rho_3$  and  $\theta_3$  also are initially excited [Figs. 9(c) and 9(d)]. In the second case, there are small peaks corresponding to the frequencies of the hydrogen atom. This coupling with the other degrees of freedom increases only slightly at the higher temperature. Moreover, the absence of the spectral lines at low frequency should be noted: the dynamics of  $u_2$  seems not to be affected significantly by the slow energy exchange.

### B. Long-time energy exchanges

In order to look at the efficiency of the intramolecular dipole-charge interaction as an energy transduction mechanism we also excited differently two contiguous zones of the chain, and checked if there was energy exchange between the two in experiments 400 ps long. We initially excited  $u_2$ ,  $\rho_3$ ,  $\theta_3$ ,  $u_3$ ,  $\rho_4$ , and  $\theta_4$ ; the first (second) zone is the one specified by the first (second) three coordinates. Initially the energy was uniformly distributed among the degrees of freedom in one zone but different amounts of energy were given to the two zones, corresponding to different temperatures. During the runs we compared the average energy in the two zones with the initial values; and found that no appreciable flow of energy outside the initially excited region takes place. Therefore, characteristic times of a possible significant energy transfer across a molecule via the change-of-polarization mechanism simulated by the dipole-charge interaction, must be longer than 400 ps.

## IV. DISCUSSION AND CONCLUSIONS

We started this investigation with the aim of building a model for a peptide hydrogen-bonded chain. We have

neglected several of the molecular details, but the equilibrium positions determined by experiment and reasonable values for the physical constants in the calculation of the forces have been retained. The interactions we modeled provided a nonlinear coupling between the degrees of freedom we have considered, and we have studied the way in which this coupling transduces energy along the chain of molecules. The main conclusions are the following.

(i) The dynamics is quite ordered, showing regular vibrations of all degrees of freedom over very long times, even at high temperature.

(ii) Energy is widely exchanged between the stretching and the bending of a N—H bond, with a characteristic period of about 0.2 ps. This exchange is maximum when both degrees of freedom have about the same energy, and it is strongly reduced when the two degrees of freedom have very different energies.

(iii) An energy transfer through the H bond takes place between an H atom and the related O atom; this exchange is periodic (period of about 0.4 ps), is of small amplitude, and is most effective when the two molecules bound by the H bond have similar energies.

(iv) No significant energy transfer across a peptide group, via the dipole-charge interaction, was detected; characteristic times of this process should be greater than 400 ps.

(v) Energy exchange is lower and slower at lower temperatures.

Thinking of an ACN chain, attention is drawn to the phenomenon of energy trapping or soliton excitation.<sup>3,4</sup> In this context, the lack of energy diffusion across the peptide group that we observe might be of no great relevance. Indeed, we have not included in our model the vibration of the C—N linkage, which would probably provide a much more efficient coupling than its polarization. On the other hand, the characteristic features of the energy exchange through the hydrogen bond might contribute to the trapping of localized energy by hindering its flow to a neighboring molecule. This can be seen in the following way, considering the results in Figs. 6 and 7: absorption of an ir photon of  $1650\text{ cm}^{-1}$  amounts to an energy increase corresponding to  $\Delta T = hc\tilde{\nu}/k_B \simeq 2380\text{ K}$ ; let us suppose that the absorption process leads to a sudden transition in the energy of one of our vibrational degrees of freedom. If the system is initially at a temperature of 20 K, as a result of the photon absorption this degree of freedom will increase its energy to 2400 K, while the other two will stay at 20 K. The intermolecular region entailing three degrees of freedom has a total energy corresponding to 2440 K; therefore, it can be thought of as being at an average temperature of about 815 K. The initial energy being concentrated mainly on one degree of freedom, the horizontal coordinate in Fig. 7 has a value near 0 or 1; as a consequence, the exchange of energy through the hydrogen bond between the oxygen and the hydrogen in the excited region almost vanishes. Moreover, Fig. 6 shows that if the excited degree of freedom is  $\rho$  or  $\theta$ , the energy exchange between the two is also reduced. Altogether, quantumlike absorption of radiative energy modifies the dynamics of the excited region in such a way as to diminish the dispersion of this energy.

It may be noticed that this mechanism is less efficient at higher temperature. In the example given before, 98% of the average energy corresponding to about 815 K is concentrated on the excited degree of freedom. If the temperature of the system before absorption was 200 K, after the transition the average energy of the excited region would correspond to about 995 K; but the most energetic degree of freedom would account for only 87% of the energy, while each of the others would have nearly 7% of the total. Figure 7 shows that in this case the energy exchange through the hydrogen bond is only reduced by about a half with respect to the state in which equipartition holds.

Point (iii) of this section suggests a slight tendency toward self-trapping of energy even in the absence of absorbed radiation. Indeed, a thermal fluctuation which produces a local concentration of energy on few molecules diminishes the rate of energy exchange between these molecules and the rest of the chain; in other words, a thermal fluctuation tends to stabilize itself.

It seems advisable to extend our study in order to take more features of the real system into account. Work is in progress to develop a more complex model in which the molecules will be allowed to vibrate around their equilibrium positions; those low-frequency vibrations are in fact believed to play a role in the generation of a solitonic excitation in ACN.<sup>3,4</sup> An extended analysis of the energy transport along an ACN chain requires the inclusion of the C—N stretching in the model.

#### ACKNOWLEDGMENTS

We want to thank Professor G. Careri for his support and warm interest during this work. Interesting discussions with Professor A. C. Scott and Professor P. L. Christiansen are gratefully acknowledged. One of us (A.G.) thanks Professor N. N. Khuri for the kind hospitality at the Rockefeller University. This work has been partly supported under European Economic Community Contract No. STI-059-J-C (CD), and by Gruppo Nazionale di Struttura della Materia del Consiglio Nazionale delle Ricerche and by Centro Interuniversitario di Struttura della Materia del Ministero della Pubblica Istruzione (Italy).

#### APPENDIX A: DIPOLE-CHARGE FORCE

The dipole is located at the center of the C—N bond; the charge excesses are positive for the hydrogen atom ( $q'$ ) and negative for the oxygen atom ( $q$ ). We get (see Fig. 2) for the dipole-charge forces acting on these two atoms

$$F_{\text{DC},u} = -\frac{2p|q|}{(u+d)^3}, \quad (A1)$$

$$F_{\text{DC},\rho} = -\frac{2p|q'|}{(\rho+d)^3}.$$

The sign of the forces refers to the axes along which the displacements  $u$  and  $\rho$  are measured;  $d$  is half the length of the C—N bond. The dipole  $p$  is generated by the

charge excesses of the two atoms, and its component along the C—N bond is

$$p = a \left[ |q| \left[ \frac{1}{(u+d)^2} - \frac{1}{(u_0+d)^2} \right] + |q'| \left[ \frac{1}{(\rho+d)^2} - \frac{1}{(\rho_0+d)^2} \right] \right], \quad (\text{A2})$$

where  $a$  is the polarizability of the bond. We have subtracted the equilibrium value of the induced dipole, which has already been taken into account in the balance of all forces which determine the equilibrium position of the atoms.

We now develop (A1) and (A2) in powers of  $u - u_0$  and  $\rho - \rho_0$  up to terms of the second order. Inserting the expansions of (A2) into the expansion of (A1) and keeping again terms up to the second order yields

$$F_{\text{DC},u}^{(i)} = \frac{4aq^2}{(u_0+d)^6} (u_i - u_0) + \frac{4a|qq'|}{(u_0+d)^3(\rho_0+d)^3} (\rho_i - \rho_0) - \frac{18aq^2}{(u_0+d)^7} (u_i - u_0)^2 - \frac{6a|qq'|}{(u_0+d)^3(\rho_0+d)^4} (\rho_i - \rho_0)^2 - \frac{12a|qq'|}{(u_0+d)^4(\rho_0+d)^3} (u_i - u_0)(\rho_i - \rho_0),$$

$$F_{\text{DC},\rho}^{(i)} = \frac{4aq'^2}{(\rho_0+d)^6} (\rho_i - \rho_0) + \frac{4a|qq'|}{(u_0+d)^3(\rho_0+d)^3} (u_i - u_0) - \frac{18aq'^2}{(\rho_0+d)^7} (\rho_i - \rho_0)^2 - \frac{6a|qq'|}{(u_0+d)^4(\rho_0+d)^3} (u_i - u_0)^2 - \frac{12a|qq'|}{(u_0+d)^3(\rho_0+d)^4} (u_i - u_0)(\rho_i - \rho_0).$$

## APPENDIX B: HYDROGEN BONDING FORCES

In order to obtain explicit expressions for this force we write the distance between the oxygen in the  $i$ th molecule and the hydrogen in the  $(i+1)$ th molecule as a function

of  $u_i$ ,  $\rho_{i+1}$ , and  $\theta_{i+1}$  (see Fig. 1 and Table I). With the help of the Carnot theorem, a power expansion up to second order in the displacements from equilibrium positions yields the following expressions, in which again we subtracted the equilibrium values:

$$F_{\text{Hb},u}^{(i)} = \frac{3\cos^2\alpha - 1}{r_0^3} |qq'| (u_i - u_0) + \frac{2\cos\alpha |qq'|}{r_0^3} (\rho_{i+1} - \rho_0) + \frac{\rho_0 \sin\alpha |qq'|}{r_0^3} \theta_{i+1} + \frac{15\cos^2\alpha - 9}{2r_0^4} \cos\alpha |qq'| (u_i - u_0)^2 + \frac{3\cos\alpha}{r_0^4} |qq'| (\rho_{i+1} - \rho_0)^2 - \frac{3\rho_0^2 + 2\rho_0 r_0}{2r_0^4} \cos\alpha |qq'| \theta_{i+1}^2 + \frac{9\cos^2\alpha - 3}{r_0^4} |qq'| (u_i - u_0)(\rho_{i+1} - \rho_0) + \left[ \frac{1}{r_0^3} + \frac{3\rho_0}{r_0^4} \right] \sin\alpha |qq'| \theta_{i+1} (\rho_{i+1} - \rho_0) + \frac{3\rho_0 \sin 2\alpha}{r_0^4} |qq'| (u_i - u_0) \theta_{i+1},$$

$$F_{\text{Hb},\rho}^{(i)} = \frac{2}{r_0^3} |qq'| (\rho_i - \rho_0) + \frac{2\cos\alpha}{r_0^3} |qq'| (u_{i-1} - u_0) + \frac{3}{r_0^4} |qq'| (\rho_i - \rho_0)^2 + \frac{9\cos^2\alpha - 3}{2r_0^4} |qq'| (u_{i-1} - u_0)^2 - \frac{3\rho_0^2 + 4\rho_0 r_0 + r_0^2}{2r_0^4} |qq'| \theta_i^2 + \frac{6\cos\alpha}{r_0^4} |qq'| (\rho_i - \rho_0)(u_{i-1} - u_0) + \left[ \frac{1}{r_0^3} + \frac{3\rho_0}{r_0^4} \right] \sin\alpha |qq'| (u_{i-1} - u_0) \theta_i,$$

$$F_{\text{Hb},\theta}^{(i)} = -\frac{\rho_0^2 + \rho_0 r_0}{r_0^3} |qq'| \theta_i + \frac{\rho_0 \sin\alpha}{r_0^3} |qq'| (u_{i-1} - u_0) + \frac{3\rho_0 \sin 2\alpha}{2r_0^4} |qq'| (u_{i-1} - u_0)^2 + \left[ \frac{1}{r_0^3} + \frac{3\rho_0}{r_0^4} \right] \sin\alpha |qq'| (\rho_i - \rho_0)(u_{i-1} - u_0) - \frac{3\rho_0^2 + 4\rho_0 r_0 + r_0^2}{r_0^4} |qq'| (\rho_i - \rho_0) \theta_i - \frac{3\rho_0^2 + 2\rho_0 r_0}{r_0^4} \cos\alpha |qq'| (u_{i-1} - u_0) \theta_i.$$

- <sup>1</sup>For a review see A. S. Davydov, Usp. Fiz. Nauk. **138**, 603 (1982) [Sov. Phys.—Usp. **25**, 898 (1982)].
- <sup>2</sup>G. Careri, in *Cooperative Phenomena*, edited by H. Haken and M. Wagner (Springer, Berlin, 1973).
- <sup>3</sup>G. Careri *et al.*, Phys. Rev. B **30**, 4689 (1984).
- <sup>4</sup>For a comprehensive article, see A. C. Scott, Philos. Trans. R. Soc. London A **315**, 423 (1985).
- <sup>5</sup>G. Careri and J. Wyman, Proc. Natl. Acad. Sci. U.S.A. **81**, 4386 (1984); **82**, 4115 (1985).
- <sup>6</sup>See Ref. 3 for details for the spectroscopic band assignment.
- <sup>7</sup>J. F. Olsen and S. Kang, Theor. Chim. Acta **17**, 329 (1970).
- <sup>8</sup>See J. C. D. Brand and J. C. Speakman, *Molecular Structure* (Arnold, London, 1960).
- <sup>9</sup>A. T. Hagler, E. Huler, and S. Lifson; J. Am. Chem. Soc. **96**, 5319 (1974).
- <sup>10</sup>L. Verlet; Phys. Rev. **159**, 98 (1967).